Improvement of interferometric SAR coherence estimates by slope-adaptive range common-band filtering

Maurizio Santoro, Charles Werner, Urs Wegmüller
Gamma Remote Sensing
CH-3073 Gümligen, Switzerland
[santoro, cw, wegmuller]@gamma-rs.ch

Oliver Cartus
Department of Earth Observation
Friedrich-Schiller University
D-07743 Jena, Germany
Oliver.Cartus@uni-jena.de

Abstract—**The accuracy of SAR interferometric coherence estimates depends on the precision of several processing steps. In particular decorrelation can occur if range common-band filtering does not perform optimally. Typically a planar surface is adopted which introduces additional decorrelation in case of sloped terrain. To take into account topographic variations a slope-adaptive range common-band filtering method has been developed. A DEM is used to simulate an unwrapped interferogram and the fringe rate is used as driver for the filter size in the range common-band filtering step. Tests with several spaceborne interferometric SAR datasets confirmed the robustness of the method. The improvement of the coherence increased for increasing perpendicular baseline. As a consequence, the fringe visibility also greatly improved. To quantify the improvement of the coherence estimates with the slope-adaptive range common-band filtering, we considered the variation of classification in forest mapping, i.e. an application in which accurate coherence estimates are needed. With improved coherence the classified forest stem volume agreed better with forest maps derived from other remote sensing datasets.**

Keywords-SAR interferometry; coherence; range common-band filtering; slope; forest; phase unwrapping.

I. INTRODUCTION

Correct estimation of the interferometric SAR coherence plays a crucial role in several applications of the coherence itself as well as of the interferometric phase. For forest biomass retrieval for example, even a slight error in the coherence estimate can lead to an estimate of biomass having a relevant deviation from the actual value. The uncertainty of the interferometric phase estimate is strictly linked to the corresponding coherence level, which in turn means that decorrelation introduced by the processing chain could lead to substantial errors when estimating terrain elevation, displacements etc. Furthermore, the robustness of phase unwrapping is enhanced if the coherence is increased.

The generation of a SAR coherence image requires several processing steps, namely co-registration of two images, common-band filtering in range and azimuth, and estimation of the coherence. Each step is in practice associated with decorrelation, in the sense that if a step is not performed correctly, decorrelation is either introduced or retained.

Common-band filtering in range (also referred to also as wavenumber shift filtering, [1]) has been conceived to compensate for spatial decorrelation in the range direction. Because of the spatial separation in space of the two SAR antennas, the ground reflectivity spectra of the two images present a certain offset. The offset depends on the length of the perpendicular component of the interferometric baseline. For increasing length, the overlap of the spectra decreases. The spatial decorrelation resulting from the partial overlap of the ground reflectivity spectra can be compensated for by filtering out the parts of the spectra which are not common to the two images. Often range common-band filtering assumes a flat planar surface, thus implying that the filtering is not fully correct in the case of sloped terrain. As a consequence, coherence is underestimated. The effect is enhanced for longer perpendicular component of the baseline.

To take into account topographic features in the compensation for spatial decorrelation, we consider an approach based on topographic phase simulated from a DEM for the range common-band filtering. Section 2 describes the processing methodology. Section 3 presents a summary of the results for a number of test cases. Section 4 illustrates how specific applications benefit from the improved range common-band filtering approach.

II. COHERENCE ESTIMATION BASED ON SLOPE-ADAPTIVE RANGE COMMON-BAND FILTERING

The SAR interferometric coherence is estimated from two SAR images in Single Look Complex format (g_1 and g_2) using an ensemble average over a window of finite size (N samples). To take into account phase variations due to topographic variations, the estimation includes a geometry and topography-induced phase modulation term $e^{-j\phi}$ (see (1)).

When a DEM is available, it is possible to get to a precise description of the phase modulation term at high spatial resolution, thus enhancing the accuracy of the coherence estimate. If the DEM is not available, it is possible to derive this term from the interferogram itself or use an approximation in which the phase is described by either a constant, linear, quadratic or higher order function over the estimation window. Depending on the chosen slope function, the correction changes the statistics of the estimator and influences the accuracy of the coherence estimates (cf. [2]).

$$|\hat{\gamma}| = \frac{\left|\sum_{i=1}^{N} g_{1,i} g_{2,i}^{*} e^{-j\varphi_i}\right|}{\sqrt{\sum_{i=1}^{N} |g_{1,i}|^2 \sum_{i=1}^{N} |g_{2,i}|^2}} \quad (1)$$

The numerator in (1) can also be expressed as the product of the magnitude of the two co-registered SLCs and the differential interferogram. Hence if in the differential interferometric processing the common-band filtering retains uncorrelated part of the spectra of the two images or the elevation information in the DEM presents some errors (e.g. undersampling of slopes, noise) decorrelation is introduced.

When range common-band filtering assumes a flat planar surface, spatial decorrelation is introduced on sloped areas. The decorrelation increases for increasing perpendicular baseline length since the overlap of the spectra decreases. To go around the problem without having the need to change the common-band filters, we considered compensating the interferometric phase by using a simulated interferogram from elevation information, such as a DEM. The estimate of the local fringe rate in the simulated interferogram is used to determine the slope-dependent spectral shift and therefore the filter length. Since the simulated interferometric phase is generated from a DEM and a baseline model, it allows compensation at high resolution, the effect being particularly significant for image pairs characterized by long baselines.

III. SAR Data and Interferometric Processing

The traditional and the slope-adaptive range common-band filtering procedure have been used to generate coherence images for several spaceborne SAR datasets. Here we present a summary of the results in order to highlight the sensitivity of the coherence estimation procedure to

1. length of perpendicular baseline;
2. DEM resolution given an interferometric pair.

The examples we have selected to further illustrate these points refer to data acquired by ERS-1/2 SAR over the provinces of Jilin and Liaoning in Northeast China (43.6º N, 124.7º E and 40.1º N, 122.3º E respectively). This is part of the extensive Forest DRAGON Project dataset used to map forest cover and forest biomass in Northeast China [3]. Both image frames include a wide range of topographic features, from completely flat ground to steep mountain slopes. The main land use for flat areas includes agricultural fields and urban settlements. Mountain slopes are predominantly bare.

Table 1 lists the interferometric pairs with respect to test area, acquisition date, perpendicular baseline, B_n, and DEM used for the generation of the differential interferogram. To simulate the unwrapped interferometric phase necessary for processing SRTM-3 elevation data were used. For the Jilin frame, SRTM-1 X-band data were also available, thus allowing the comparison of coherence images for different DEM resolutions.

For processing multi-look factors of 1 and 5 in range and azimuth respectively were used to decrease noise, resulting in 20x20 m^2 pixel size. To obtain accurate coherence estimates without loosing too much in resolution we used an adaptive coherence estimation method with window size varying between 3x3 and 9x9. To allow inter-comparisons images were finally geocoded to 25x25 m^2 pixel size.

TABLE I. List of interferometric pairs.

Area	Date	B_n (m)	DEM
Liaoning	1996-01-18/19	149	SRTM-3
Liaoning	1996-02-22/23	40	SRTM-3
Liaoning	1996-03-28/29	102	SRTM-3
Jilin	1996-01-15/16	390	SRTM-3
Jilin	1996-01-15/16	390	SRTM-1

IV. Processing Results

To illustrate the sensitivity of the different processing methods to baseline length, we consider the Liaoning dataset. Figure 1 illustrates the effect of aspect angle on the coherence of bare soils for different slope angles. For steep slopes facing the radar (~ 100º) the coherence decreased because of increasing foreshortening and layover effects. By using the slope-adaptive range common-band filtering, the coherence increased (see lower plots in Figure 1), the increase being stronger at longer baselines.

The improvement of the coherence estimates on sloped terrain when using the slope-adaptive method becomes clearer for even longer baseline compared to those found at Liaoning. The Jilin image pair has a rather long perpendicular baseline (390 m, i.e. one third of the ERS critical baseline). Figure 2 shows that the coherence greatly improved on sloped terrain when slopes are taken into account in the range common-band filtering procedure. Figure 2a and b show the coherence images obtained without and with slope-adaptive range common-band filtering and based on the SRTM-3 DEM. The increase of coherence due to the slope-adaptive range common-band filtering is not only visible in these two plots but also in Figure 2e where the difference between the improved coherence and the original coherence has been displayed. Comparison with the DEM in Figure 2d confirms that coherence mostly improved on sloped terrain.

Figure 2 also shows that the coherence further improved when a DEM with higher resolution was used. The coherence in Figure 2c is based on the SRTM-1 DEM and shows slightly higher coherence on sloped terrain. This result becomes clearer when looking at Figure 2f, which shows the difference between this coherence image and the one based on the SRTM-3 DEM in Figure 2b. The effect of using DEMs with different spatial resolutions (SRTM 1 arcsec versus SRTM 3 arcsec data) shows an improvement of the coherence estimate by using the narrow-scale DEM in areas of rapid changes of topography. However, we could also notice a slight decay of the coherence due to the noisier quality of the X-band SRTM-1 DEM compared to the SRTM-3 DEM.

Although not showed here, the use of a slope-adaptive range common-band filtering approach in the interferometric processing of pairs with long baselines implies less noisiness of the interferometric phase observations and therefore more reliable phase unwrapping, more accurate estimate of terrain elevation and possibility to better detect terrain displacements.

V. Coherence-Based Thematic Mapping

The improvement of the approach to coherence estimation is here demonstrated with an example on land-cover and forest mapping. ERS-1/2 SAR tandem coherence data are known for being a reliable observable in terms of forest/non-forest mapping because of the much higher coherence of unvegetated areas with respect to vegetated areas. If decorrelation occurs, e.g. due to uncompensated spatial decorrelation, bare surfaces can be erroneously classified as forests. In Figure 3 we illustrate for the Jilin dataset the result of forest stem volume classification based on the coherence obtained with and without the slope-adaptive range common-band filtering approach using SRTM-3 DEM. The classification method has been described in [4]. By using the improved coherence image, 7.5% of all pixels were classified as having lower stem volume, including bare ground, because of the higher coherence following the improved coherence estimation. Only for 2% of the pixels the classification resulted in an increase of stem volume. The results are in better agreement with the information provided by other satellite remote sensing data (MODIS land cover product, MODIS Vegetation Continuous Fields product).

VI. Conclusions

In this paper we have illustrated a method for improving coherence estimates over sloped terrain using slope-adaptive range common-band filtering. Tests were conducted for a number of spaceborne SAR datasets. For image pairs with long baselines (at least 30% of the critical baseline) coherence was improved significantly over sloped terrain. As a consequence, the fringe visibility of the differential interferogram in such areas was also improved. On the other hand the coherence estimates for pairs with short baselines (approximately up to 10% of the critical baseline) remained practically unchanged. The improved coherence estimation method has significant implications, e.g. for land cover applications such as forest mapping. Improved coherence estimation reduces misclassification of bare ground and low biomass forests. Furthermore, by increasing the coherence the robustness of phase unwrapping is enhanced and the estimation of terrain elevation and displacements is improved.

Acknowledgment

ERS-1/2 SAR data have been obtained through ESA's Cat-1 Projects 2553 (Forest Dragon) and 1333. The SRTM-1 dataset has been obtained from DLR-DFD.

References

[1] F. Gatelli, A. Monti Guarnieri, F. Parizzi, P. Pasquali, C. Prati, and F. Rocca, "The wavenumber shift in SAR interferometry," *IEEE Trans. Geosci. Remote Sensing*, vol. 32, pp. 855-865, 1994.

[2] P. B. G. Dammert, "Accuracy of INSAR measurements in forested areas," *Proc. 'Fringe 96' Workshop on ERS SAR Interferometry*, Zürich, 30 September - 2 October, 1996.

[3] M. Santoro, O. Cartus, C. Schmullius, U. Wegmüller, C. Werner, A. Wiesmann, Y. Pang, and Z. Li, "On the generation of a forest biomass map for Northeast China: SAR interferometric processing and development of classification algorithm," *Proc. Fringe 2005 Workshop*, ESA-ESRIN, Frascati, 28 November - 2 December, 2005.

[4] O. Cartus, M. Santoro, C. Schmullius, P. Yong, and Z. Li, "Creation of large area forest biomass maps for Northeast China using ERS-1/2 tandem coherence," *Proc. ENVISAT Symposium*, Montreux, 23-27 April, 2007.

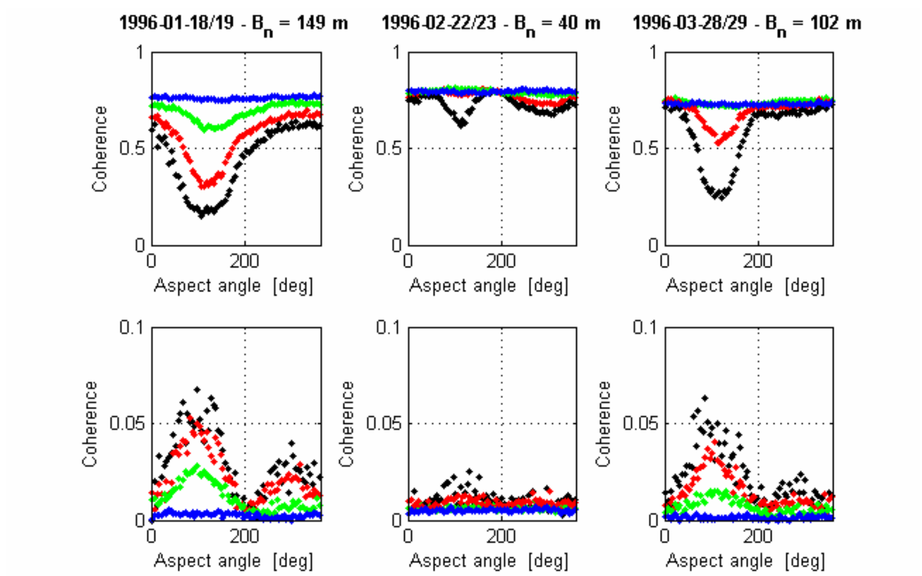

Figure 1. Coherence as a function of aspect angle for the Liaoning image frame (above) and difference between coherence obtained with and without slope-adaptive range common-band filtering (below). Results are showed for four different slope angles (blue = 0°, green = 5°, red = 10°, black = 15°).

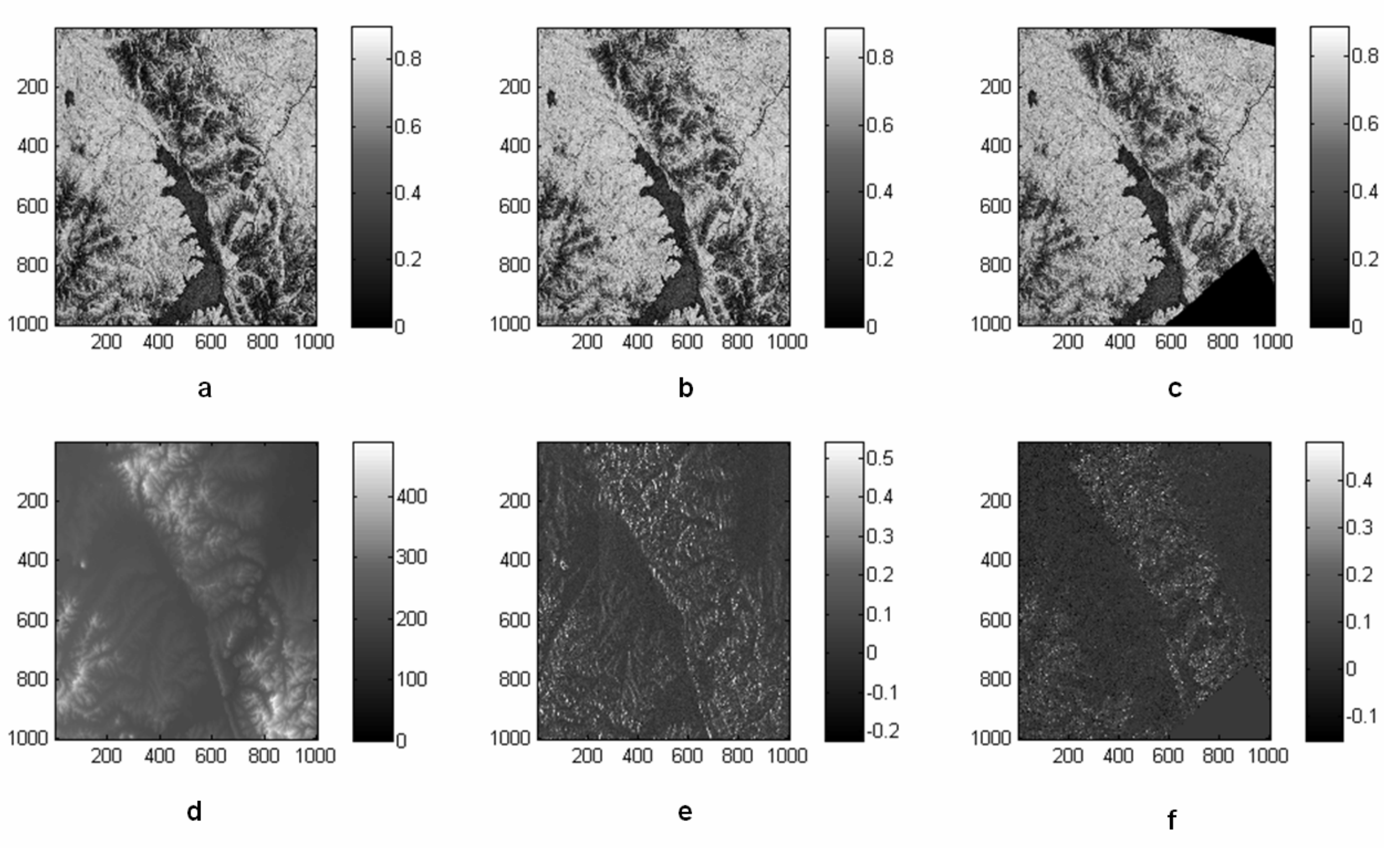

Figure 2. Coherence images obtained without and with slope-adaptive range common-band filtering based on SRTM-3 (a and b), and with slope-adaptive common-band filtering based on SRTM-1 DEM (c). SRTM-3 DEM (d), image difference b-a (e), image difference c-b (f).

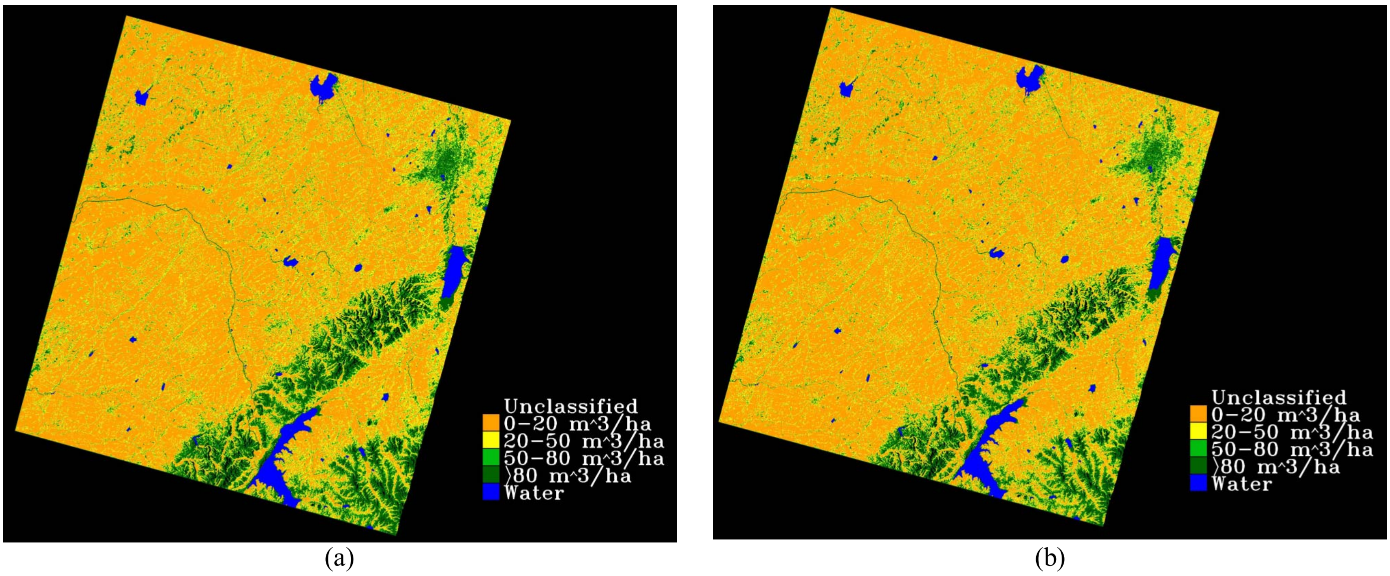

Figure 3. Classified forest stem volume in m^3/ha using coherence (a) without and (b) with slope-adaptive range common-band filtering. In (b) forested regions have lower biomass or are classified as bare ground (instead of forest) because of the increased coherence after slope-adaptive range common-band filtering.